International Journal of Environmental Sciences
ISSN: 2229-7359
Vol. 11 No. 7, 2025
https://www.theaspd.com/ijes.php

The Model Order Reduction For The Load Frequency Control Of Two Area Power System Network Using Genetic Algorithm And Pole Clustering

[1]**Hariom Rawal,** [1]**Tanveer Ahmad Wani,** [2]**Jay Singh**
[1]Noida International University Greater Noida,U.P, India
[2]G.L. Bajaj Institute of Technology & Management, Greater Noida,U.P, India

Abstract– *The article presents the model order reduction of the load frequency control (LFC) of the multi-area or two area power system network using genetic algorithm (GA) and pole clustering method. Load disturbance causes persistent frequency deviations in the multi-area or two-area power system network which have an impact on other parameters. The complete system has been developed by considering various generating units of each area such as solar photovoltaic (SPV), wind turbine (WT), battery energy (BESS), and conventional source (CS) which are connected through AC grid. The system has been modelled in terms of transfer function and the order of the overall transfer function is too high. It is need to reduce the order of transfer function which will be assessed separately for both numerator and denominator. The coefficient of denominator of the transfer function has been determined by using pole clustering method and coefficient of numerator of the transfer function has been determined by using genetic algorithm. The performance of frequency deviation is analysed using performance measures like integral square error (ISE), integral absolute error (IAE), and integral time absolute error (ITAE). To analyse the frequency deviation with 1% disturbances, a network of two area power systems has also been established. For the 1% disturbances in the two-area model, GA achieves the lowest frequency deviation and least mechanical deviation in contrast to the traditional technique. In addition to this, ISE, IAE and ITAE are also found to be minimum with GA in contrast to higher order system. This all shows the superiority of GA for reducing the model order reduction.*
Keywords–*GA, LFC, ISE, IAE, ITAE*

INTRODUCTION

One of the main issues that investigators deal with is nonlinearity analysis using a straightforward method. Most real-time systems are either linear or non-linear systems. The order of the systems that are both linear and non-linear is too high. Real-time systems are usually expressed in terms of higher order differential systems. The larger order system, which is typically expressed using differential equations, must therefore have its order reduced. By lowering the larger order system to a reduced order system, the LFC of a two area power system network has been evaluated. This technique has been evaluated by using the pole clustering method to reduce the coeff. of the transfer function's denominator, as well as a genetic algorithm to calculate the coeff. of the transfer function's numerator.

A thorough model order reduction approach is presented in this research to facilitate quick system-level energy integrity verification. This method was created to restrict models of entire power delivery systems of high-end systems with multiple processors, in which closed-loop electrical board as well as package models are linked to chip algorithms and loads via banks of per-core Fully Integrating Voltage Regulator. A straight transient simulation at the system level is extremely difficult because of the intricacy of the dynamics and the quantity of signals that need to be tracked. We demonstrate that a thorough topology structure for the circuit equ. results in a global model format that makes it possible to eliminate the unnecessary states using a structured projection framework [1].

The LFC problem is presented in this study as a huge-scale system control problem and as a typical rejection of disturbances problem. For this reason, a straightforward method of LFC design for power systems with load disturbance and unpredictability of parameters is suggested. The method relies on an altered IMC filter design as well as a two's-degree-of-freedom intern. model control system that unifies the concepts of model-order reduction such as the Routh and Padé estimates. In order to mitigate load disruptions, this technique improves the closed-loop system response. To demonstrate the effectiveness as well as effectiveness in terms of resilience & optimal performance, the suggested method is implemented in a

MATLAB program for a single producing unit with non-reheated turbines in an one-area power system [2].

Instead of revealing the PFR dynamics corresponding to every generation unit, this study demonstrates how all units impact frequency changes from the perspective of the system reaction. Making a set of data in order to identify the PFR model, just the system frequencies is required, resulting in sparse measurements. Real observations of an actual power system as well as computer models of a test system with various unit types are used to confirm the efficacy of the suggested approach [3].

This letter suggests a method for estimating the center of inertia's frequency that relies solely on bus frequency measurements, such as those found in phasor measurements, the network's admittance matrix, as well as two synchronous generator parameters—the internal response and the inertia constant. The suggested formula requires a much smaller set of bus frequency measurements and can be used online [4].

The idea of frequency security margin is put forth in this work in order to measure the system's capacity to regulate frequency in the event of an emergency. It is the greatest power unbalance that the system can withstand while maintaining a frequency that is within the acceptable range. A model for frequency restricted unit commitment that takes frequency security margin into account is put forth. Initially the system frequencies nadir is analytically formulated while taking into account the frequ. supports from VRE plants as well as the frequency control properties of the thermal generators. The rate security margin is then individually transformed after being analytically formulated [5].

From the standpoint of stability of frequency, the optimal placement of virtual inertia is viewed in this article as a techno-economic issue. First, an analogous representation of battery energy storage devices as viewed from the electrical system is put forth, based on facts. Through the use of the virtual inertia idea, this empirically verified model enhances inertial response by utilizing the unique characteristics of the energy storage system. In order to improve frequency responsiveness while maintaining a minimal storage capacity, a fresh structure is then put forth that takes into account the characteristics of the battery storage system, such as longevity, yearly costs, and state of charge, while determining the best placement [6].

In [7], it was demonstrated how to use the OOBO algorithm to control terminal voltage & load frequencies in an actual four-area multi-source connected power system with nonlinearities.

With regard to the physical limitations of governors dead-band (GDB) & generating rate constraint (GRC), the proposed hybrid dynamic framework is presented for one area of a multi-unit electrical system comprising gas, reheat thermal, and hydro units. Under a 0.01 pu step load disruption, the proposed hybrid dynamical framework simultaneously adjusts the settings of the CPSS and LFC loop using an improved PSO method. Furthermore, the system's dynamic responses to a small-signal disruption in the baseline voltage of the AVR are evaluated. Simulation findings indicate that the LFC system's dampening effectiveness is enhanced by the usage of this hybrid model since the CPSS successfully lowers the area reduced frequency oscillations[8].

This paper examines the joint study of LFC and automated voltage regulation (AVR) for multi-area combination systems. As an alternative, the conventional PID controller is employed. A novel differential development artificial electric field algorithm (DE-AEFA) for modifying parameters of controllers is proposed in this study. The DE-AEFA methods are first used to test system 1, which is made up of two-area non-reheat turbines that generate steam. subsequently, the research is extended to a combination model called test system 2 with the goal to investigate the combination LFC and AVR problem. Furthermore, an HVDC link is added to the system along with the existing AC tie-line. The main element that enhances system reactivity is AC/DC, not merely AC tie-line [9].

This paper presents a new coordinated control method for simultaneous voltage and frequency stabilizing in a multi-area the system. A unique differential evolution-artificial electric field (DE-AEFA) method is suggested for tweaking the classical PID as a regulator. By contrasting its unpredictable responses with those of alternative algorithms, the DE-AEFA-based regulate system's feasibility is confirmed using a widely used test method of a dual area heat capacity with turbines of non-reheat framework. In addition, the shifting reactions of the system under discussion have been examined by placing interline power flow controllers (IPFC) in tie-line redox flow battery packs (RFBs) in both locations. This work shows the benefits of IPFC and RFBs in lowering frequency, tie-line, and voltage anomalies through cooperation with the proposed controller [10].

Optimal power flow (OPF) is a constrained multi-objective, non-linear issue. The computationally demanding nature of evolutionary algorithms (EAs) to obtain a globally distributed & uniformly distributed Pareto front (PF) makes OPF problems costly. Thus, in order to solve the OPF problem, a hybrid two-phase approach combined with a parameter-less constraint method is used. The suggested method finds better convergence and equally distributed PF by combining single and multi-objective EAs. The suggested approach is validated and tested on IEEE 30 and 300-bus networks using a variety of conflicting objective functions. Twenty separate runs of each example are performed. Fuzzy decision-making is used to determine the best-compromised the solution, and the hyper volume indication technique is used to get the optimal PF [11].

Using a novel multi-objective optimization framework, this paper presents a nonlinear threshold acceptance heuristic. For a two-area electrical system, this technique is used to choose the control gains of a linked AVR-LFC scheme in order to guarantee steady and quick AC generator bus voltage-frequency regulation in response to dynamic disturbances. This method optimizes competing objective criteria while determining a set of control laws that provide quick dynamic responsiveness. Along with additional analytical techniques like internal model-control methods, it is validated against other common heuristics, such as ABC, DE & PSO [12].

In this work, we framework disturbances and uncertainty in parameters into the LFC model to offer an adaptive supplementary control strategy for the power system's frequency control. For the LFC problem, a new sliding control variable is specifically recommended, and the basic controller is an enhanced sliding mode control (SMC). The additional control signal is provided by the adaptable dynamic programming technique, which helps with frequency regulation by adjusting to unpredictability as well as disturbances in real time. To ensure the dependability of the suggested control strategy, a stability analysis is also supplied. In contrast, an SMC technique based on PSO is created as the best variable controller for the frequency control issue [13].

To maintain a steady frequency and guarantee the dependability of power systems, LFC, is crucial. The LFC problem is made more difficult by the widespread use of sporadic but sustainable sources like solar and wind. Furthermore, the LFC problem is further complicated by the power systems' generating rate constraint. This study discusses an integral SMC approach for wind turbine-powered power systems with regard to the restriction. Sliding-mode-based neural networks are used to estimate the uncertainties of electricity systems because the interruption of wind farms as well as the linearization of GRC worsen the unpredictability. The Lyapunov direct approach is used to calculate the neural networks' weight update formulas. The LFC problem is solved using the neural-network-based integral sliding mode controller [14].

Grid codes develop a sophisticated and stringent frequency recovery criterion (FRC) to guarantee that contemporary power systems can withstand frequency excursions following a power outage. This research suggests a real-time adaptive load shedding technique for receiving-end power systems' frequency recovery control, per the FRC. For intelligent load shedding control, a load shedding controller based on the co-active neuro-fuzzy inference system (CANFIS) is created. While the shedding quantity at the present shedding round and the time delay of the subsequent round are used as control signals, the bus frequency's magnitude deviation and recovery time deviation are derived based on the FRC and employed as feedback signals [15].

VARIOUS PERFORMANCE PARAMETERS

The integral square error(ISE) has been mathematically represented in Eq.1 [13].

$$\text{ISE} = \int_0^\infty [\text{g(t)-r(t)}]^2 \qquad (1)$$

The unit response of original model & reduced order model are represented by $g(t), r(t)$

$$IAE = \int_0^\infty | g(t) - r(t) | dt \qquad (2)$$

$$ITAE = \int_0^\infty t | g(t) - r(t) | dt \qquad (3)$$

The parameters like integral absolute error(IAE), and integral time absolute error(ITAE) have been mathematically expressed in Eq.2 and Eq.3. [13]

TWO AREA POWER SYSTEM NETWORK

It has been suggested that the multi-area system is an interconnected system of two-area electrical systems. There are interconnected loads, connected grids, SPV, WT, and BESS in each network of power systems area. Figure 1 depicts the structure of the whole composite made up of different generating units.

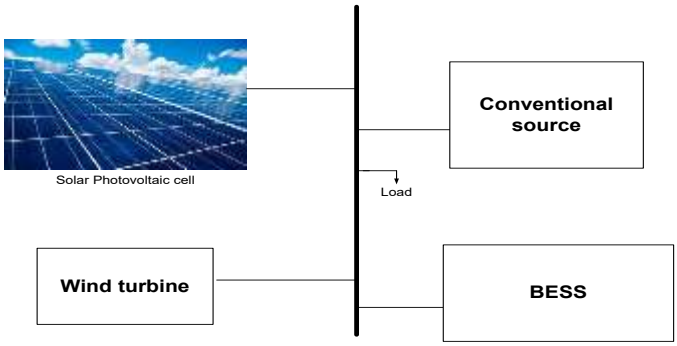

Fig.1 Structure of the proposed model

In general, solar and wind disturbances happen frequently during the day. The output power is also impacted by these disruptions or oscillations, which ultimately results in a shift in both frequency as well as power. Similar fluctuations or variations will be seen in the output from other producing sources, including BESS and traditional sources. To analyze such oscillations, their generating sources are expressed as a transfer function. The multi-area system function transfer model is derived from [17]. Equation 4, which can be expressed mathematically in a general way, shows how the frequency deviation of the two area system affects the line dividing the flow of electricity between two regions of the power system network.

$$\Delta P_{tie,a} = \frac{2\pi T_{ab}}{s}(\Delta F_a - \Delta F_b) \quad (4)$$

'a' and 'b' are the two areas respectively. According to Equation 5, the distinction between different generating units and load is transmitted through a first-order system, which results in a deviation in the frequency of area "a."

$$(\Delta P_{sa} + \Delta P_{wa} + \Delta P_{ba} + \Delta P_{ga} - \Delta P_{da})\frac{k_{pa}}{1+T_{pa}} = \Delta F_a \quad (5)$$

As stated in Equation 6, the disturbance determines the variation in solar photovoltaic output.

$$\Delta P_{sa} = \frac{k_{sa}}{1+T_{sa}}\Delta d_{sa} \quad (6)$$

As stated in Equation 7, the input disruption determines the change in wind turbine output.

$$\Delta P_{wa} = \frac{k_{wa}}{1+T_{wa}}\Delta d_{wa} \quad (7)$$

As stated in Eq. 8, the frequency deviations determine how the BESS output changes.

$$\Delta P_{ba} = \frac{k_{ba}}{1+T_{ba}}\Delta F_a \quad (8)$$

The way an area's area control is altered depends on power variations and frequency fluctuations. Ideally, this power & frequency shift will be close to zero. In general, ACE depends on deviations in frequency as well as power, which are coupled linearly and are provided in Eq. 9.

$$ACE = \beta_a \Delta F_a + \Delta P_{tie,a} \quad (9)$$

Eq.10 illustrates how this ACE alters the power generation of a traditional source by passing via a FO-PID controller and a specific transfer function gain.

International Journal of Environmental Sciences
ISSN: 2229-7359
Vol. 11 No. 7, 2025
https://www.theaspd.com/ijes.php

$$\Delta P_{ga} = \frac{1}{(1+sT_{ga})(1+sT_{ga})}(k_p + \frac{k_i}{s^{\mu}} + s^{\lambda}k_d)ACE_a \quad (10)$$

Using the random hit-and-trial approach, the proportionality constant of the FO-PID controller is found to be Kp = 2.5, Ki = 5.2, Kd = 5.7, λ = 1.2, and μ = 2.6. Figure 2 depicts the general configuration of the two-area power system network as a transfer function model of different generating units.

ΔP_{sa} , ΔP_{wa} , $\Delta P_{ba,}$ $\Delta P_{ga.}$ ΔP_{da} are the respective change in power of solar photovoltaic of area 'a', change in power of wind turbine of area 'a', change in power of BESS of area 'a', change in power of conventional generating units of area 'a', change in power of load of area 'a'.

Δd_{wa} , Δd_{sa} and ΔF_a is the change in disturbance due to wind and solar photovoltaic and frequency deviation of the area 'a' respectively.

K_{sa}, K_{ba}, k_{wa}, are the gains of solar photovoltaic, BESS, wind turbine respectively. T_{sa}, T_{ba}, T_{wa} is the time constant of solar photovoltaic, BESS, wind turbine respectively.

ACE are the area error of the area 'a' and 'b' respectively.

Similarly, all the above-mentioned terminologies can be used for the second area 'b'. The typical representation of two area system is shown in Fig.2 using

TRANSFER FUNCTION OF THE ORGINAL SYSTEM

Fig. 2 is a refer0ence to the layout of the two area power system network. There is a detailed description of each standard parameter required to build the two area network. In the two-area system, ΔFa indicates the frequency change in area 1, while ΔFb indicates the frequency change in area 2. The mathematical expression of change in frequency deviation for the area 'a' (ΔF_a) can be found in Eq. 11.

$$\Delta F_a = \frac{\frac{k_{sa}}{1+T_{sa}}\Delta d_{sa} + \frac{k_{wa}}{1+T_{wa}}\Delta d_{wa} + \frac{1}{(1+sT_{ga})(1+sT_{ga})}(k_p + \frac{k_i}{s^{\mu}} + s^{\lambda}k_d)ACE_a - \Delta P_{da}}{1 - \frac{k_{ba}}{1+T_{ba}}} \quad (11)$$

In the Eq.11, λ = 1.2, and μ = 2.6 which makes the expression of Eq.11 of five degree.

In the similar way, the mathematical expression of change in frequency deviation for the area 'b' (ΔF_b) can be found in Eq. 12.

$$\Delta F_b = \frac{\frac{k_{sb}}{1+T_{sb}}\Delta d_{sb} + \frac{k_{wb}}{1+T_{wb}}\Delta d_{wb} + \frac{1}{(1+sT_{gb})(1+sT_{gb})}(k_p + \frac{k_i}{s^{\mu}} + s^{\lambda}k_d)ACE_b - \Delta P_{db}}{1 - \frac{k_{bb}}{1+T_{bb}}} \quad (12)$$

In the Eq.12, For the same value of λ and μ which also makes the expression of Eq.12 of five degree.

It is seen that frequency deviation of the two-area system is of high order so it is required to reduce the order of the system

MODEL ORDER REDUCTION OF HIGH ORDER LOAD FREQUENCY CONTROL SYSTEM

Since it is observed that order of transfer function of frequency deviation of area 'a' and area 'b' are high so that it is required to reduce the order of the transfer function. The coefficient of denominator of the transfer function has been determined by using pole clustering method and coefficient of numerator of the transfer function has been determined by using genetic algorithm.

5.1) Pole clustering method

Both for real and imaginary poles, pole clusters are created from the initial high order system [18]. For moderately stable systems, the simplified models must preserve the poles on the imaginary axis..

5.1.1 For real poles: Let 'z' represent the number of poles in a cluster that has actual poles, such as $(p_1, p_2, ..., p_z)$, then an algorithm that is computer-oriented can be expressed as

Step-1: Set $j = 1$

Step-2: Determine the center of the pole cluster based on the poles. { $|p_1| < |p_2| < ... |p_z|$ }

International Journal of Environmental Sciences
ISSN: 2229-7359
Vol. 11 No. 7, 2025
https://www.theaspd.com/ijes.php

$$p_{cj} = -\left[\left(\sum_{i=1}^{z}\sqrt{|p_j|}\right) \div z\right]^2 \qquad (11)$$

Step-3: Counter increment as $j = j+1$

Step-4: Determine the centre of the pole cluster based on the poles z as shown in Eq.12

$$p_{cj} = -\left[\left(\sqrt{|p_{c(j-1)}|} + \sqrt{|P_1|}\right) \div 2\right]^2 \qquad (12)$$

Step-5: If $j = z+1$,

Consequently, the ultimate effective pole cluster center is $p_{ej} = p_{cj}$, then go to *Step-3*

5.1.2 For complex poles: Examine a cluster of poles with only intricate conjugate poles, like $[(\alpha_1 \pm j\beta_1),(\alpha_2 \pm j\beta_2),\ldots,(\alpha_m \pm j\beta_m)]$ The same approach discussed in Step 1 may then be used to independently determine the efficient complex cluster center (Ac ±jBc) for the imaginary & real components of the pole.

Where, $\overset{*}{p}_e = A_c + jB_c$ and $\overset{\bullet}{p}_e = A_c - jB_c$

Following the acquisition of the effective cluster places, one of the subsequent situations [18] may result in the reduced denominator of the order.:

5.1.2.1 The decreased k^{th}-order denominator could be attained, if the pole cluster centre could be real as in Eq.13 $D_k(s) = (s-p_{e1})(s-p_{e2})\ldots(s-p_{ek})$ (13)

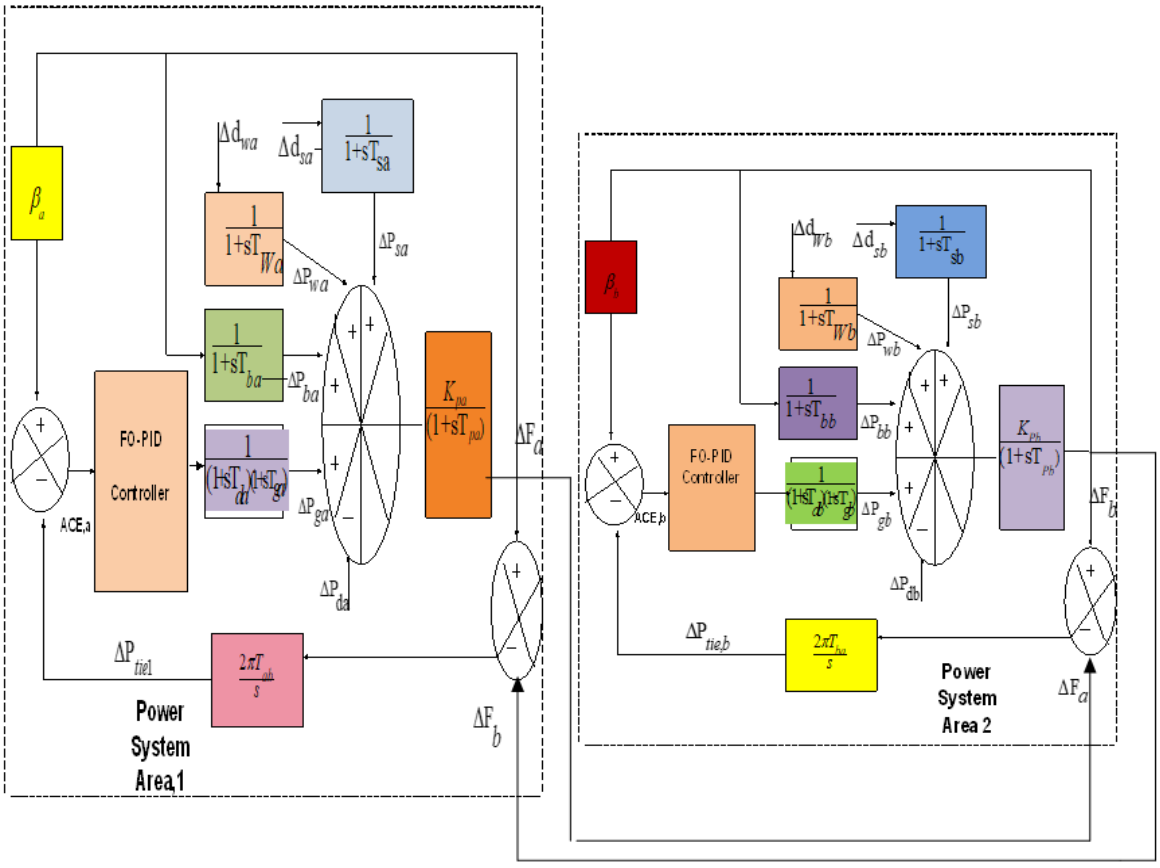

Fig.2 LFC of two area network

5.1.2.2: Eq. 14 can be produced if cluster centers are real and one cluster center pair is a complex conjugate. $$D_k(s) = (s - p_{e1})(s - p_{e2})...(s - p_{e(k-2)})(s - \overset{*}{p}_{e1})(s - \overset{\bullet}{p}_{e1}) \quad (14)$$

5.1.2.3: Eq. 15 can be achieved if every pole cluster center is a complex conjugate.

$$D_k(s) = (s - \overset{*}{p}_{e1})(s - \overset{\bullet}{p}_{e1})(s - \overset{*}{p}_{e2})(s - \overset{\bullet}{p}_{e2})...(s - \overset{*}{p}_{ek/2})(s - \overset{\bullet}{p}_{ek/2}) \quad (15)$$

5.2) Genetic Algorithm

After estimating the numerator coefficients of the transfer function using pole clustering method. Then, denominator
coefficients of the transfer function will be estimated using genetic algorithm. The numerator coefficients will be multiplication of transfer function (ΔF) and denominator which can be mathematically expressed as in Eq.16

$$f(\Delta F, p_i, A_i, B_i) = num(s) = \sum_{i=1}^{n} \Delta F((s-p_i)+(s-A_i+jB_i)) \quad (16)$$

The genetic algorithm(GA) is another optimization technique for controlling or training the unidentified parameters of the transfer function. The genetic algorithm consists of three steps: reproduction, crossover, as well as mutation.
For reproduction, the best strings from the available string mating pools will be selected. Crossover is employed after replication, which causes the two best strings to switch bits.
A mutation, that is a random change from 1 to 0 or 0 to 1 at a predefined location, then occurs in a particular string.
Equation 17 provides the goal function, which essentially consists of four unknown variables.

$$f_1 = f(\Delta F, p_i, A_i, B_i) \quad (17)$$

The GA trains the objective function, and a flowchart, as seen in Fig. 3, also explains the process of implementing the genetic algorithm.
The choice of a standard variable based on the requirement for an objective function
Number of people in the population: 7
String length 5
Probability of the crossover, Pc = 0.85
Probability of the mutation, Pm = 0.07
We will use the equation found in Equation 18 to estimate these five variables

$$f_1^r = f_1^{\min} + \frac{f_1^{\max} - f_1^{\min}}{2^l - 1} y^r \quad (18)$$

where 'r' is iteration, y^r is the binary string length.
Use Equation (19) to find the new constraint variables.

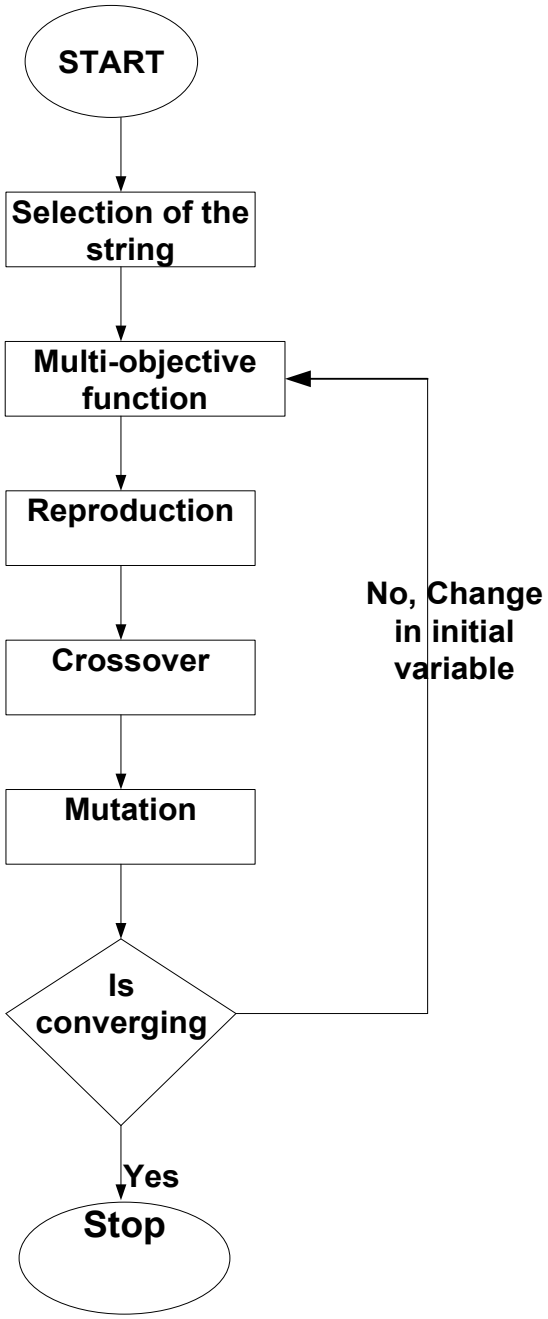

Fig.3 Flowchart explaining the process of genetic algorithm

.

$$(f^r)_{new} = \frac{1}{(1+\frac{\alpha^{'}\varepsilon^r}{f^r})} \quad (19)$$

$\alpha^{'}$ (step size)=0.55

The convergence value is shown in Eq.7

$$\varepsilon^r = \mathrm{F}(\mathrm{R}_2(\mathrm{s}))^r - \mathrm{F}(\mathrm{R}_2(\mathrm{s}))^{ref} \quad (20)$$

VI. PERFORMANCE PARAMETERS ANALYSIS AND COMPARISON

The integral square error (ISE), integral absolute error (IAE), and integral time absolute error (ITAE) have been estimated for the reduced order system using genetic algorithm(GA) and original higher order system is shown in Table.1

Table.1 Comparative analysis of performance parameter with conventional and PSO

Performance parameter	GA	Higher order system
ISE	1.29×10^{-2}	2.65×10^{-4}
IAE	4.12×10^{-2}	6.66×10^{-3}
ITAE	3.99×10^{-3}	7.56×10^{-4}

Performance metrics such as ISE, IAE, and ITAE are shown to be lower with GA for reduced order system in contrast to the original higher order system.

6.1 Effect on frequency deviation and mechanical deviation for the 1% solar disturbances:

In this section, Effect on frequency deviation and mechanical deviation for the 1% solar disturbances by keeping wind disturbance unchanged. The expression of frequency deviation for variable solar disturbances and fixed wind disturbance for the area 'a' and area 'b' are shown in Eq.21 and Eq.22

$$\Delta F_a = \frac{\frac{k_{sa}}{1+T_{sa}}\Delta d_{sa} + \frac{1}{(1+sT_{ga})(1+sT_{ga})}(k_p + \frac{k_i}{s^{\mu}} + s^{\lambda}k_d)ACE_a - \Delta P_{da}}{1 - \frac{k_{ba}}{1+T_{ba}}} \quad (21)$$

$$\Delta F_b = \frac{\frac{k_{sb}}{1+T_{sb}}\Delta d_{sb} + \frac{1}{(1+sT_{gb})(1+sT_{gb})}(k_p + \frac{k_i}{s^{\mu}} + s^{\lambda}k_d)ACE_b - \Delta P_{db}}{1 - \frac{k_{bb}}{1+T_{bb}}} \quad (22)$$

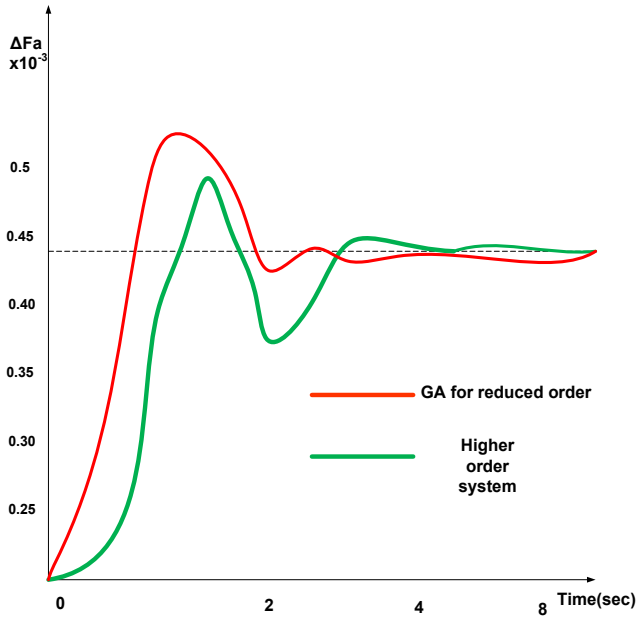

Fig.4 frequency deviation in area a due to the 1% of solar disturbance in area b

International Journal of Environmental Sciences
ISSN: 2229-7359
Vol. 11 No. 7, 2025
https://www.theaspd.com/ijes.php

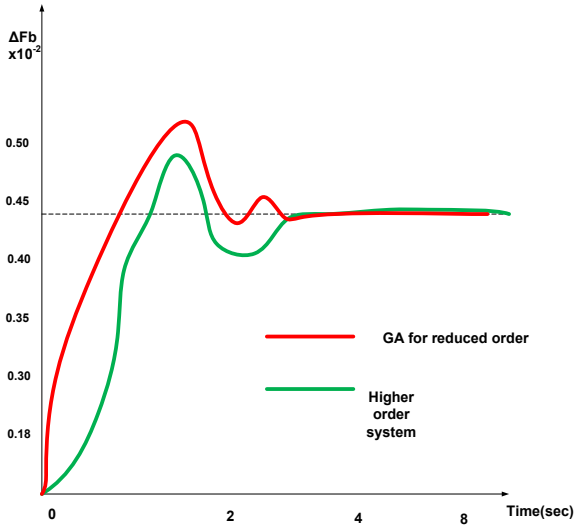

Fig.5 frequency deviation in area 'b' due to the 1% of solar disturbance in area a

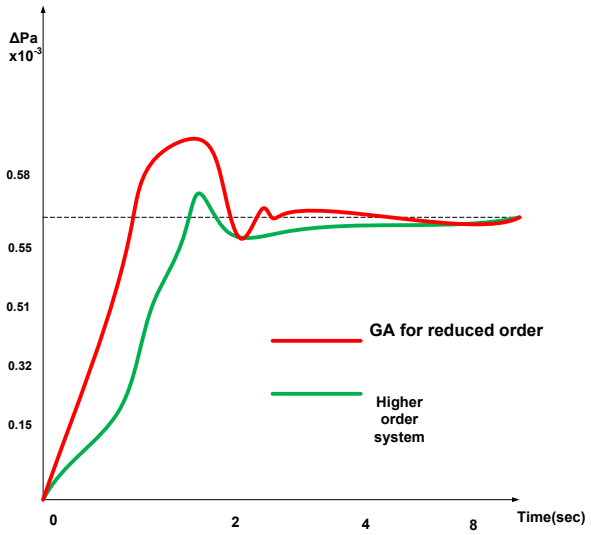

Fig.6 mechanical power deviation in the area a due to the 1% of solar disturbance in area b

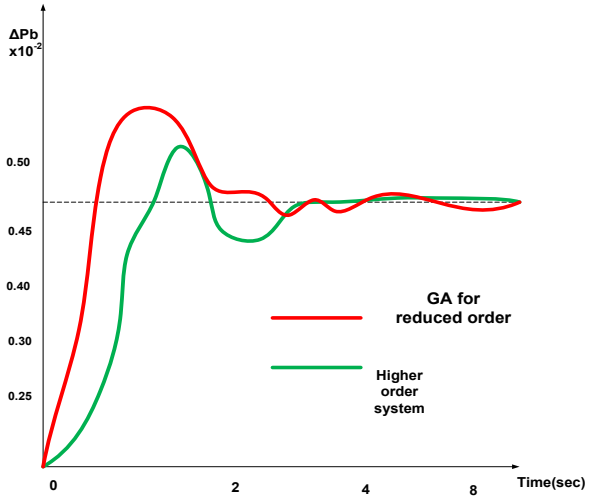

Fig.7 mechanical power deviation in the area b due to the 1% of solar disturbance in area a

International Journal of Environmental Sciences
ISSN: 2229-7359
Vol. 11 No. 7, 2025
https://www.theaspd.com/ijes.php

The frequency variation is caused by 1% solar disturbances in both areas a and b of the two-area system. Figure 4 illustrates the 1% of solar disturbance in area b cause a shift in frequency in area a. Similarly, Fig. 5 illustrates the frequency change in region b as a result of a 1% disturbance in area a. Figure 6 illustrates how a 1% disturbance in area a cause the mechanical deviation in area 'b'. Figure 7 illustrates how a 1% disturbance in area 'b' cause the mechanical deviation in area 'a'. It is generally noted that GA for reduced order reduction produces a least frequency deviation and minimum mechanical power deviation in area 'a' and area 'b' under 1% disturbances in contrast to higher order system.

6.2 Effect on frequency deviation and mechanical deviation for the 1% wind disturbances:

In this section, Effect on frequency deviation and mechanical deviation for the 1% wind disturbances by keeping solar disturbance unchanged. The expression of frequency deviation for variable wind disturbances and fixed wind disturbance for the area 'a' and area 'b' are shown in Eq.23 and Eq.24

$$\Delta F_a = \frac{\frac{k_{wa}}{1+T_{wa}}\Delta d_{wa} + \frac{1}{(1+sT_{ga})(1+sT_{ga})}(k_p + \frac{k_i}{s^{\mu}} + s^{\lambda}k_d)ACE_a - \Delta P_{da}}{1 - \frac{k_{ba}}{1+T_{ba}}} \quad (23)$$

$$\Delta F_b = \frac{\frac{k_{wb}}{1+T_{wb}}\Delta d_{wb} + \frac{1}{(1+sT_{gb})(1+sT_{gb})}(k_p + \frac{k_i}{s^{\mu}} + s^{\lambda}k_d)ACE_b - \Delta P_{db}}{1 - \frac{k_{bb}}{1+T_{bb}}} \quad (24)$$

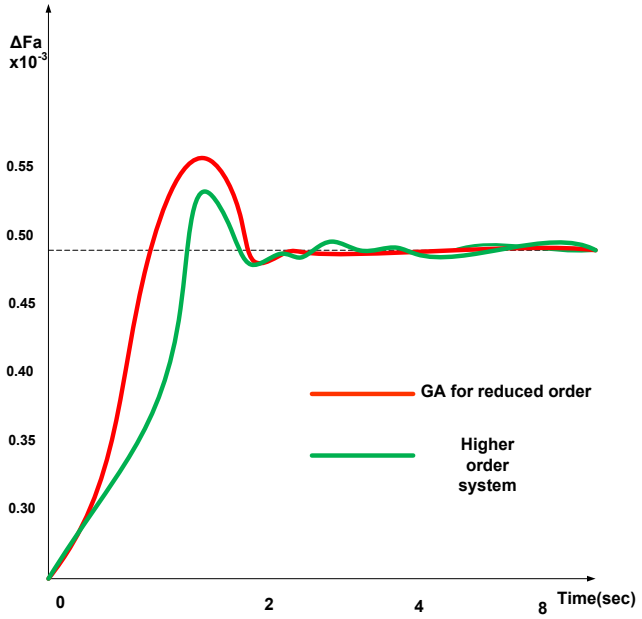

Fig. 8 frequency deviation in area a due to the 1% of wind disturbance in area b

International Journal of Environmental Sciences
ISSN: 2229-7359
Vol. 11 No. 7, 2025
https://www.theaspd.com/ijes.php

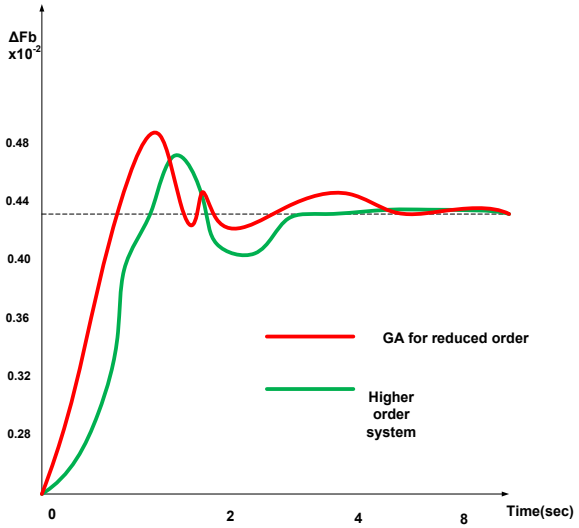

Fig.9 frequency deviation in area 'b' due to the 1% of wind disturbance in area a

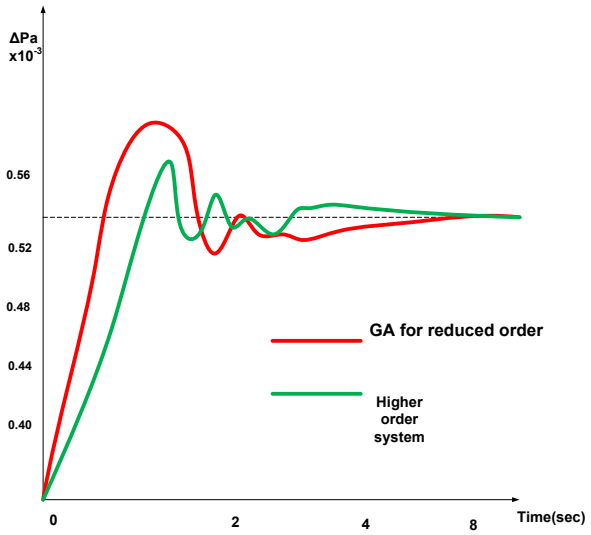

Fig.10 mechanical power deviation in the area a due to the 1% of wind disturbance in area b

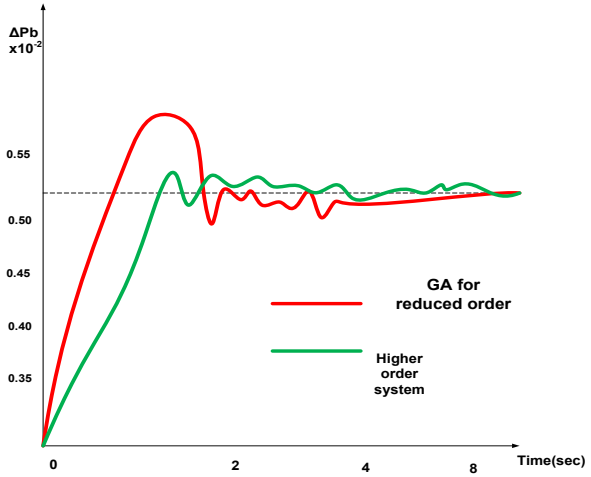

Fig.11 mechanical power deviation in the area b due to the 1% of wind disturbance in area a

In both areas a and b of the two-area system, 1% wind disturbances are the cause of the frequency fluctuation. The 1% wind disturbance in area b that results in a frequency shift in area an is depicted in Figure 8. Similarly, a 1% wind disturbance in area a causes a frequency change in region b, as shown in Fig. 9. The mechanical deviation in area "b" is caused by a 1% wind disturbance in area "a," as shown in Fig. 10. The mechanical deviation in area "a" is caused by a 1% wind disturbance in area "b," as shown in Fig. 11. It is commonly known that, in comparison to higher order systems, GA for lower order reduction results in the least frequency deviation and smallest mechanical power deviation in areas "a" and "b" under 1% wind disturbances.

CONCLUSION

The article introduces the use of genetic algorithms (GA) and pole clustering method to reduce the model order of the load frequency control (LFC) of the multi-area or two area power system network. In the multi-area or two-area power system network, load disturbance results in recurring frequency deviations that affect other parameters. A variety of generating units from each region, including solar photovoltaic (SPV), wind turbine (WT), battery energy (BESS), and conventional source (CS), which are connected via the AC grid, were taken into consideration when developing the entire system. The transfer function has been used to model the system, and the overall transfer function's order is excessively high. The transfer function's order must be lowered because it will be evaluated independently for the numerator and denominator. Using performance measures such as integral square error (E), integral absolute error (IAE), and integral time absolute error (ITAE), the frequency deviation performance is analyzed. A network of two area power systems has also been established to analyze the frequency deviation with 1% disturbances. The pole clustering method was used to determine the coefficient of denominator of the transfer function, and a genetic algorithm was used to determine the coefficient of numerator. Compared to the conventional method, GA achieves the lowest frequency deviation and the least mechanical deviation for the 1% disturbances in the two-area model. Furthermore, compared to traditional methods, GA is reported to have the lowest levels of ISE, IAE, and ITAE. All of this demonstrates how effective GA is at lowering the model order reduction.

REFERENCES

[1] Antonio Carlucci,Stefano Grivet-Talocia,Siddharth Kulasekaran, Kaladhar Radhakrishnan, Structured Model Order Reduction of System-Level Power Delivery Networks, IEEE Access, vol.12, pp. 18198 – 18214, 2024

[2] Sahaj Saxena,Yogesh V. Hote, Load Frequency Control in Power Systems via Internal Model Control Scheme and Model-Order Reduction, IEEE Transactions on Power Systems, vol.28, no..3, 2749 – 2757, 2013

[3] Bo Wang,Shishuai Zhu,Guowei Cai,Deyou Yang,Zhe Chen,Jin Ma,Zhenglong Sun, Sparse Measurement-Based Modelling Low-Order Dynamics for Primary Frequency Regulation, IEEE Transactions on Power Systems, vol.39,no.1, pp 681 – 692, 2024

[4] F. Milano, "Rotor speed-free estimation of the frequency of the center of inertia," IEEE Trans. Power Syst., vol. 33, no. 1, pp. 1153–1155, Jan. 2018.

[5] Z. Zhang, E. Du, F. Teng, N. Zhang, and C. Kang, "Modeling frequency dynamics in unit commitment with a high share of renewable energy," IEEE Trans. Power Syst., vol. 35, no. 6, pp. 4383–4395, Nov. 2020.

[6] H. Golpîra, A. Atarodi, S. Amini, A. R. Messina, B. Francois, and H. Bevrani, "Optimal energy storage system-based virtual inertia placement: A frequency stability point of view," IEEE Trans. Power Syst., vol. 35, no. 6, pp. 4824–4835, Nov. 2020

[7] Tayyab Ali,Muhammad Asad,Ezzeddine Touti,Besma Bechir Graba,Mouloud Aoudia,Ghulam Abbas,Hammad Alnuman,Waleed Nureldeen, Terminal Voltage and Load Frequency Control in a Real Four-Area Multi-Source Interconnected Power System With Nonlinearities via OOBO Algorithm, IEEE Access, vol.12, pp. 123782 – 123803, 2024

[8] J. Morsali and Z. Esmaeili, ''Proposing a new hybrid model for LFC and AVR loops to improve effectively frequency stability using coordinative CPSS,'' in Proc. 28th Iranian Conf. Electr. Eng. (ICEE), Tabriz, Iran, Aug. 2020, pp. 1–7, doi: 10.1109/ICEE50131.2020.9260695.

[9] C. N. S. Kalyan and G. S. Rao, ''Frequency and voltage stabilisation in combined load frequency control and automatic voltage regulation of multiarea system with hybrid generation utilities by AC/DC links,'' Int. J. Sustain. Energy, vol. 39, no. 10, pp. 1009–1029, Nov. 2020.

[10] C. N. S. Kalyan and G. S. Rao, ''Combined frequency and voltage stabilisation of multi-area multisource system by DE-AEFA optimised PID controller with coordinated performance of IPFC and RFBs,'' Int. J. Ambient Energy, vol. 43, no. 1, pp. 3815–3831, Dec. 2022.

[11] A. Ali, G. Abbas, M. U. Keerio, M. A. Koondhar, K. Chandni, and S. Mirsaeidi, ''Solution of constrained mixed-integer multi-objective optimal power flow problem considering the hybrid multi-objective evolutionary algorithm,'' IET Gener., Transmiss. Distrib., vol. 17, no. 1, pp. 66–90, Jan. 2023.

[12] N. Nahas, M. Abouheaf, M. N. Darghouth, and A. Sharaf, ''A multiobjective AVR-LFC optimization scheme for multi-area power systems,'' Electric Power Syst. Res., vol. 200, Nov. 2021, Art. no. 107467.
[13] C. Mu, Y. Tang, and H. He, ''Improved sliding mode design for load frequency control of power system integrated an adaptive learning strategy,'' IEEE Trans. Ind. Electron., vol. 64, no. 8, pp. 6742–6751, Aug. 2017.
[14] D. Qian, S. Tong, H. Liu, and X. Liu, ''Load frequency control by neuralnetwork-based integral sliding mode for nonlinear power systems with wind turbines,'' Neurocomputing, vol. 173, pp. 875–885, Jan. 2016.
[15] Hao Yang,Bo Jin,Zhaohao Ding,Zhenglong Sun,Cheng Liu,Dongfeng Yang,Guowei Cai,Jian Chen, Reinforcement Learning Based Adaptive Load Shedding by CANFIS Controllers for Frequency Recovery Criterion-Oriented Control, IEEE Transactions on Power Systems, vol.40, no.1, pp. 996 – 1009, 2025
[16] Afzal Sikander & Rajendra Prasad,' Soft Computing Approach for Model Order Reduction of Linear Time Invariant Systems', Circuits, Systems, and Signal Processing,Vol.34,pp,3471-3485,2015
[17] Hongyue Li , Xihuai Wang, And Jianmei Xiao, Adaptive Event-Triggered Load Frequency Control for Interconnected Microgrids by ,Observer-Based Sliding Mode Control, IEEE Access,vol. pp. 68271 – 68280,2019
[18] C.B. Vishwakarma, R. Prasad. MIMO System Reduction using modified pole clustering and genetic algorithm. Modelling and simulation in Engineering. 2009; 2009;1-9.